

# Conformational Changes of the Noncrystalline Chains for Syndiotactic Polypropylene as a Function of Temperature: Correlations with the Crystallizations of Form I and Form III

Yasumasa Ohira and Fumitaka Horii\*

*Institute for Chemical Research, Kyoto University, Uji, Kyoto 611-0011, Japan*

Takahiko Nakaoki

*Faculty of Science and Technology, Ryukoku University, Otsu, Shiga 520-2194, Japan*

*Received August 17, 2000; Revised Manuscript Received January 2, 2001*

**ABSTRACT:** The conformation and molecular mobility of the noncrystalline chains for syndiotactic polypropylene (sPP) samples well crystallized have been characterized at different temperatures by high-resolution solid-state  $^{13}\text{C}$  NMR spectroscopy. The purposes are to investigate the cause inducing the high *trans* fraction of sPP chains in the noncrystalline state just after quenched at 0 °C from the melt and to know some correlation with the crystallization of form III with the planar zigzag conformation around 0 °C. Two samples containing form I and III crystallites were respectively crystallized at 100 °C for 24 h and at 0 °C for 144 h from the melt, their degrees of crystallinity being 0.60 and 0.31. A new line shape analysis for the  $\text{CH}_2$  resonance line confirms in good accord with the previous analysis for the  $\text{CH}_3$  line that the *trans* fraction is of the high level of 0.80 in the noncrystalline state just after quenched at 0 °C from the melt. The *trans* fraction is also determined for the noncrystalline components in the form I and III samples as a function of temperature by the line shape analysis for the  $\text{CH}_3$  resonance line. As a result, it is found that there are three temperature regions, regions A, B, and C, where the *trans* fractions are greatly different. In region A below 15 °C, the *trans* fraction is as high as 0.73–0.80, and it seems to significantly depend on the degree of crystallinity. In contrast, this fraction is as low as about 0.57 in region C above 60 °C, in good accord with the level at the melt. In region B at 15–60 °C, the *trans* fraction drastically changes as is possibly named as *trans-rich chain assembly-coiled chains* transition. However, no significant conformational change is observed for the results obtained at different temperatures by the similar analysis for the  $\text{CH}_2$  resonance line, suggesting the preferable production of some conformations mainly due to the steric hindrance between the  $\text{CH}_3$  groups including the second and third neighbors.  $^{13}\text{C}$  spin–spin relaxation measurements for the noncrystalline component in the form I sample also reveal that the molecular motion is highly limited in regions A and B even above  $T_g$  while the rubberlike mobility is allowable in region C. On the basis of these experimental results and the previous results of the preferential crystallizations of forms I and III in these regions, some factors affecting these crystallizations are discussed.

## Introduction

In our previous papers,<sup>1–3</sup> we clarified the spontaneous crystallization process of the planar zigzag form<sup>4–11</sup> (form III) for syndiotactic polypropylene (sPP) around 0 °C by time-resolved wide-angle X-ray diffractometry, high-resolution solid-state  $^{13}\text{C}$  NMR spectroscopy, and infrared spectroscopy. In that case we also found that the *trans* fraction for the sPP chains is as extraordinarily high as 0.80 at 0 °C in the noncrystalline state before the crystallization of form III after quenched from the melt.<sup>2</sup> Since such a high *trans* fraction may be one of essential causes inducing the spontaneous crystallization of form III at 0 °C, it is very important to examine how such a high *trans* fraction is produced when quenched or just cooled from the melt. There may be some temperature region where the *trans* fraction becomes higher compared to the conventional value expected in the melt. Moreover, it is worth noting that the most stable form (form I<sup>4,5,12–19</sup>) composed of anti-chiral helices with the *ttgg* conformation is also crystallized above about 5 °C whereas form III is rapidly decreased in degree of crystallinity above 0 °C with increasing temperature.<sup>3</sup> In particular, form I and form III are almost equally crystallized in quantity at about 12 °C. This fact suggests that other factors may be

closely associated with the crystallization of form III in addition to the high *trans* fraction of the sPP chains.

In this paper, we first confirm the high *trans* fraction of the noncrystalline sPP chains at 0 °C just after quenched from the melt by analyzing the  $\text{CH}_2$  resonance line in a fully relaxed dipolar decoupling/magic angle spinning (DD/MAS)  $^{13}\text{C}$  NMR spectrum and obtain more information about the conformation before the crystallization of form III. Second, we examine the *trans* fraction of the noncrystalline sPP chains as a function of temperature. To this purpose, well-crystallized form I and III samples are employed, and the *trans* fraction is determined at each temperature as a first approximation for the noncrystalline component included in these samples because it is almost impossible to produce the real noncrystalline state for sPP in the absence of crystallites at temperatures higher than about 0 °C. Finally, we briefly discuss about factors affecting the crystallization of form I or form III at lower temperatures around 0 °C.

## Experimental Section

**Samples.** The sPP sample with racemic triad of 0.96, which was provided by Sumitomo Chemical Co. Ltd., was used without further purification. The glass transition temperature ( $T_g$ ), determined by DSC with a heating rate of 10 °C/min, was

about  $-5\text{ }^{\circ}\text{C}$ .<sup>20</sup> The noncrystalline sample was prepared by quenching a sPP film to the freezing temperature of  $\text{N}_2$  after melted for 10 min at  $170\text{ }^{\circ}\text{C}$  and cut into squares of several millimeters. The quenched sample was quickly set up to each apparatus kept at  $0\text{ }^{\circ}\text{C}$  without leaving the sample above  $0\text{ }^{\circ}\text{C}$ . The sample containing form I crystallites (form I sample) was isothermally crystallized at  $100\text{ }^{\circ}\text{C}$  for 24 h from the melt and then slowly cooled to room temperature. In contrast, the sample with form III crystallites (form III sample) was crystallized at  $0\text{ }^{\circ}\text{C}$  for 144 h from the melt and left at room temperature for several days.<sup>20</sup> The degrees of crystallinity for form I and III samples were determined to be 0.60 and 0.31 by high-resolution solid-state  $^{13}\text{C}$  NMR spectroscopy as described later, respectively.

**Solid-State  $^{13}\text{C}$  NMR Measurements.** High-resolution solid-state  $^{13}\text{C}$  NMR spectra were recorded at various temperatures ranging from  $-50$  to  $120\text{ }^{\circ}\text{C}$  on a JEOL JNM-GSX200 spectrometer equipped with a partly modified JEOL variable temperature system under a static magnetic field of 4.7 T. The  $^1\text{H}$  and  $^{13}\text{C}$  field strengths  $\gamma B_1/2\pi$  were 62.5 kHz. Each sample was spun in a zirconia rotor at a rate of 3.0 kHz. Fully relaxed DD/MAS  $^{13}\text{C}$  NMR spectra were collected with transients of 128 or 256. The pulse delay time after the acquisition of FID was set to be as long as 5 times the spin-lattice relaxation time ( $T_{1C}$ ) for the  $\text{CH}_2$  or  $\text{CH}_3$  carbon.  $^{13}\text{C}$  chemical shifts were expressed as values relative to tetramethylsilane ( $\text{Me}_4\text{Si}$ ) by using the  $\text{CH}_3$  line at 17.36 ppm for hexamethylbenzene crystals as an external reference. The sample temperature was calibrated using the temperature dependence of relative chemical shifts of  $\text{CH}_2$  and OH protons of ethylene glycol in a glass ampule, which was packed with KBr in a MAS rotor.<sup>21–23</sup>

## Results and Discussion

**Conformation of Noncrystalline sPP Chains below  $0\text{ }^{\circ}\text{C}$ .** In our previous paper,<sup>2</sup> we clarified by high-resolution solid-state  $^{13}\text{C}$  NMR analysis that the *trans* fraction is as high as 0.80 at  $0\text{ }^{\circ}\text{C}$  for the noncrystalline sPP chains just after quenched from the melt. In this analysis the  $\text{CH}_3$  resonance line was resolved into two Lorentzian lines,  $\text{CH}_3(\text{I})$  and  $\text{CH}_3(\text{II})$ , which are assigned to the  $\text{CH}_3$  carbons associated with the *tt* and *tg* (or *gt*) conformations for the  $\text{CH}_2\text{--CH}(\text{CH}_3)\text{--CH}_2$  bonds, respectively.<sup>5,7,23</sup> This analytical method was also very effective for the characterization of the spontaneous crystallization process of form III with the planar zigzag conformation<sup>2</sup> and of the crystal transformation from form III to form II composed of isochiral helices with the *ttgg* conformation.<sup>20</sup> In contrast, the  $\text{CH}_2$  resonance line, which will provide similar information about the chain conformation, was not analyzed because  $^{13}\text{C}$  spin-lattice relaxation times ( $T_{1C}$ ) for the  $\text{CH}_2$  line are rather longer compared to those of the  $\text{CH}_3$  line particularly after the crystallization. Here, we analyze the  $\text{CH}_2$  resonance line for the noncrystalline sample obtained by quenching at  $0\text{ }^{\circ}\text{C}$  from the melt to confirm the extraordinarily high *trans* fraction of the noncrystalline sPP chains at  $0\text{ }^{\circ}\text{C}$  and to obtain more detailed information about the conformation.

To suppress the crystallization of form III, the quenched sample was further cooled to  $-20\text{ }^{\circ}\text{C}$ , which is below the glass transition temperature ( $\sim -5\text{ }^{\circ}\text{C}$ ) of sPP,<sup>20</sup> and the  $T_{1C}$  relaxation process was first measured at this temperature by the CPT1 pulse sequence. Figure 1 shows the semilogarithmic  $T_{1C}$  decay plot for the  $\text{CH}_2$  resonance line. Unexpectedly, the decay curve is not described as a single exponential, but it is found to consist of two components with  $T_{1C} = 18$  and  $0.4\text{ s}$ . Although the  $\text{CH}_2$  resonance line has some structure at  $-20\text{ }^{\circ}\text{C}$  due to the different conformations as shown later, the total line shape stays almost unchanged for

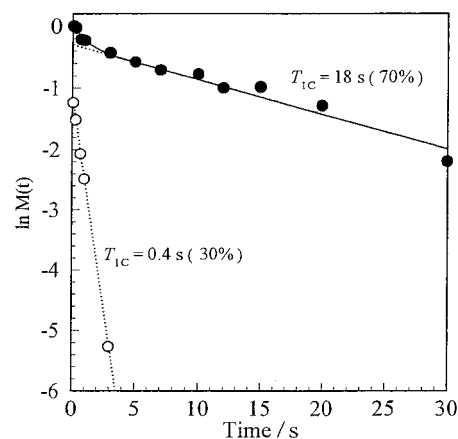


**Figure 1.**  $^{13}\text{C}$  spin-lattice relaxation behavior of the  $\text{CH}_2$  resonance line for the noncrystalline sPP sample quenched at  $0\text{ }^{\circ}\text{C}$  from the melt, measured at  $-20\text{ }^{\circ}\text{C}$  by the CPT1 pulse sequence.

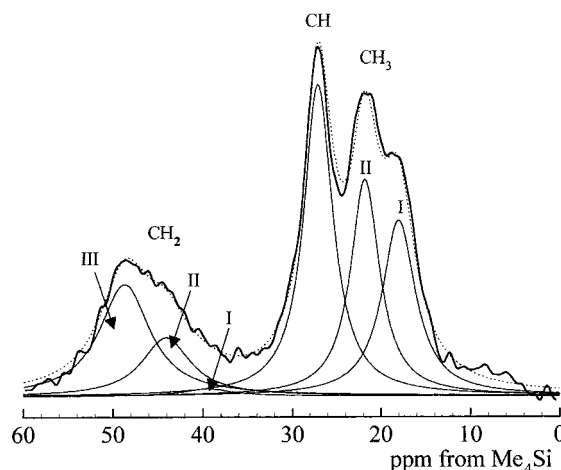


**Figure 2.** A fully relaxed DD/MAS  $^{13}\text{C}$  NMR spectrum measured at  $-20\text{ }^{\circ}\text{C}$  for the noncrystalline sPP sample quenched at  $0\text{ }^{\circ}\text{C}$  from the melt.

different  $T_{1C}$  decay times. Therefore, this fact suggests that there exists structural inhomogeneity as detected by the difference in molecular mobility associated with  $T_{1C}$  ( $\sim 10^8\text{ Hz}$ ) even before the crystallization of form III.

On the basis of the  $T_{1C}$  analysis, a fully relaxed DD/MAS  $^{13}\text{C}$  NMR spectrum of the quenched sPP sample was measured at  $-20\text{ }^{\circ}\text{C}$  by using the  $\pi/2$  single pulse sequence with a pulse delay time of 90 s. Figure 2 shows the DD/MAS  $^{13}\text{C}$  NMR spectrum (thick solid curve) thus obtained. The  $\text{CH}_3$  resonance line is found to be again successfully resolved into the  $\text{CH}_3(\text{I})$  and  $\text{CH}_3(\text{II})$  lines in good accord with the result at  $0\text{ }^{\circ}\text{C}$  described above. Here, the  $\text{CH}$  line seems to be described by a single Lorentzian, because the  $\text{CH}$  carbon is always subjected to the  $\gamma$ -gauche effect of the same level from the  $\text{CH}$  or  $\text{CH}_3$  carbon at the  $\gamma$ -position irrespective of the *trans* or *gauche* conformation. In contrast, the  $\text{CH}_2$  resonance line may be resolved into three lines,  $\text{CH}_2(\text{I})$ ,  $\text{CH}_2(\text{II})$ , and  $\text{CH}_2(\text{III})$ , which are respectively assignable to the *g@g*, *t@t* (or *g@t*), and *t@t* for the  $\text{CH}_2\text{--CH}(\text{CH}_3)\text{--CH}_2$  sequence by considering the extent of the  $\gamma$ -gauche effect. Here, @ indicates *t* or *g*. According to the analytical result for the  $\text{CH}_3$  line described above, there is no contribution from the *gg* conformation for the  $\text{CH}_2\text{--CH}(\text{CH}_3)\text{--CH}_2$  sequence probably owing to the steric hindrance. This fact indicates that lines II and III for the  $\text{CH}_2$  carbons should be ascribed to the



**Figure 3.** Schematic structure model for the noncrystalline sPP chains just after quenched at 0 °C from the melt.

following specified conformations: *tttg*, *gttt*, *tgtg*, and *gtgt* for line II and *tttt*, *ttgt*, *tggt*, and *tggt* for line III. Since the *tt*, *tg*, and *gt* fractions are respectively 0.60, 0.20, and 0.20 by the analysis for the CH<sub>3</sub> line, integrated fractions of lines I, II, and III are assumed to be 0.64, 0.32, and 0.04 by the statistical calculation, respectively. In fact, the CH<sub>2</sub> line is found to be really resolved into these three lines as shown in Figure 2 by the computer-aided least-squares method. Here, the respective lines are assumed to be Lorentzians, and the chemical shifts of lines I, II, and III are fixed to 49, 44, and 39 ppm on the basis of the chemical shifts for forms I, II, III, and IV, respectively.<sup>5,7,12,17</sup> Since the integrated fractions thus obtained for lines I, II, and III are almost in good accord with the values assumed from the results for the CH<sub>3</sub> line, it can be confirmed that the *trans* fraction is really as high as 0.80 at 0 °C in the noncrystalline state just before the crystallization of form III. Moreover, it is found that the *gg* conformation is allowable for the CH(CH<sub>3</sub>)–CH<sub>2</sub>–CH(CH<sub>3</sub>) bonds in good accord with the statistical presumption based on the analytical results for the CH<sub>3</sub> line, whereas the *gg* conformation is prohibited for the CH<sub>2</sub>–CH(CH<sub>3</sub>)–CH<sub>2</sub> bonds probably owing to the steric hindrance associated with the CH<sub>3</sub> group. It should be also noted that the *tg* or *gt* conformation seems not to be prohibited for the CH(CH<sub>3</sub>)–CH<sub>2</sub>–CH(CH<sub>3</sub>) bonds in the noncrystalline region, although the previous reports<sup>5,24</sup> pointed out that it was not allowed for the crystalline sPP chains.

Figure 3 shows a structural model schematically drawn for the noncrystalline sPP backbone chains which are statistically composed of sequences assigned to lines I–III for the CH<sub>2</sub> carbons. Each chain is locally extended due to the high *trans* fraction and the low content of the vicinal *gg* conformation for the CH(CH<sub>3</sub>)–CH<sub>2</sub>–CH(CH<sub>3</sub>) bonds. Such a situation will be preferable to the initiation of the crystallization of form III with the planar zigzag conformation. Some aggregates of the *trans*-rich segments may be also produced at 0 °C at the lapse of time in the noncrystalline region, and they should interrupt the further crystallization of form III at 0 °C or the additional crystallization of form I composed of antichiral helices with the *ttgg* conformation when annealed at room temperature.<sup>2</sup> It should be, however, noted here that such a highly *trans*-rich conformation will not be allowed for single chains but for assemblies of chains probably through the intermolecular interaction.

**Conformation Changes of the Noncrystalline Chains as a Function of Temperature.** It is impossible to examine the *trans* fraction of the noncrystalline sPP chains at temperatures above about 0 °C because the crystallization of form III or form I should occur

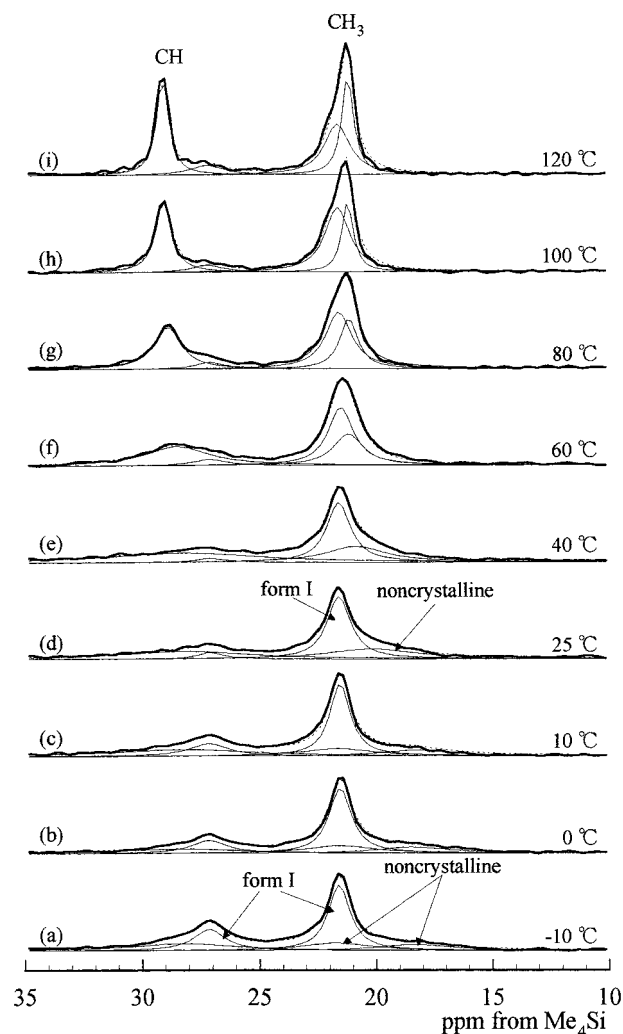


**Figure 4.** Fully relaxed DD/MAS <sup>13</sup>C NMR spectra measured at different temperatures for the form I sample.

during NMR measurements. As a first approximation, therefore, we determine the *trans* fraction of the noncrystalline component included in a well isothermally crystallized sPP sample as a function of temperature. In this paper, two kinds of samples are examined: samples isothermally crystallized for 144 h at 0 °C and for 24 h at 100 °C. These samples are respectively referred to as form III and form I samples, because they selectively contain form III and form I crystallites. Somewhat more detailed description about the preparation is made in the Experimental Section.

Figure 4 shows DD/MAS <sup>13</sup>C NMR spectra for the form I sample at different temperatures ranging from –10 to 120 °C. Observed curves are denoted as thick solid lines, and only CH and CH<sub>3</sub> resonance lines are shown in this figure for simplicity. The *T*<sub>1ρ</sub> values for the CH<sub>3</sub> carbons was found to be less than 1 s above 0 °C, although it was 2.4 s at –10 °C. By considering these values, the pulse delay time for the  $\pi/2$  single pulse sequence was set 5 s above 0 °C or 12 s at –10 °C. Therefore, fully relaxed resonance lines are obtained for the CH<sub>3</sub> carbons at the respective temperatures.

As is clearly seen in this figure, the line shape of the CH<sub>3</sub> resonance line is markedly changed with increasing temperature. To make such changes clearer, the same line shape analysis employed for the characterization of the crystal transformation of form III in a previous

paper<sup>20</sup> is also applied to this case. It should be here noted that the selective observation of the noncrystalline component by the  $T_{1C}$  filtration method is almost impossible for the  $\text{CH}_3$  resonance line in sPP samples because there is no significant difference in  $T_{1C}$  between the crystalline and noncrystalline contributions. Below 10 °C, the  $\text{CH}_3$  resonance line seems to be resolved into three Lorentzian lines. The relatively narrower line at about 22 ppm should be assigned to the  $\text{CH}_3$  carbons in the form I crystallites, because the chemical shift corresponds to the *tg* conformation for the  $\text{CH}_2\text{--CH}(\text{CH}_3)\text{--CH}_2$  sequence.<sup>2,20</sup> In contrast, two broader lines appearing at about 22 and 18 ppm are ascribed to the noncrystalline component with the *tg* and *tt* conformations, respectively.<sup>2,20</sup> As for the CH resonance line in this temperature range, the crystalline and noncrystalline contributions are simply described by two Lorentzians with different line widths. It should be additionally pointed out that the relative intensities of the CH constituent lines do not reflect their mass fractions because the CH line is partially relaxed one due to the long  $T_{1C}$  for the crystalline component.

According to the results of the line shape analysis of the  $\text{CH}_3$  resonance line below 10 °C, the degree of crystallinity of form I is determined to be 0.60 as integrated fraction for the form I component appearing at about 22 ppm. It is also found that the integrated fractions of the  $\text{CH}_3(\text{I})$  and  $\text{CH}_3(\text{II})$  lines for the noncrystalline component are 0.46–0.47 and 0.54–0.53, respectively. This fact leads to the conclusion that the *trans* fraction of the noncrystalline component is 0.73–0.74 below 10 °C for the form I sample, which seems somewhat lower than the value (0.80) in the noncrystalline state at 0 °C just after quenched from the melt.

Above 25 °C, the two noncrystalline  $\text{CH}_3$  lines clearly merge into a single line, and the line width significantly becomes narrower with increasing temperature. According to the two-site exchange model,<sup>25</sup> the *t*–*g* exchange rate is estimated to be about 100 Hz at 10–25 °C. Moreover, the single noncrystalline line evidently shifts downfield with the increase of temperature, whereas the chemical shift of the crystalline component stays constant in this temperature region. By using the two-site exchange model,<sup>25</sup> the *trans* fraction is estimated to  $0.72 \pm 0.02$ – $0.57 \pm 0.02$  for the noncrystalline component in the form I sample above 25 °C as explicitly shown in a figure later.

The CH resonance line above 25 °C can be also resolved into two Lorentzian curves similarly to the case below 10 °C. However, marked motional narrowing is observed for the noncrystalline component with increasing temperature after rather indistinct motional broadening at lower temperatures. Since the widest line seems to be observed at 25 °C, the rate of molecular motion associated with the change in line width may attain to the order of the  $^1\text{H}$  dipolar decoupling field ( $\sim 10^5$  Hz) at this temperature.<sup>26–29</sup> The contribution from the crystalline component for the CH line is still greatly suppressed due to the long  $T_{1C}$  value above 25 °C.

As for the form III sample, the line shape analysis of the  $\text{CH}_3$  and CH resonance lines was already carried out at 30–120 °C to characterize the crystal transformation and structural changes of form III induced at this temperature range in a previous paper.<sup>20</sup> On the basis of this analytical result, the *trans* fraction of the noncrystalline chains in the form III sample can be

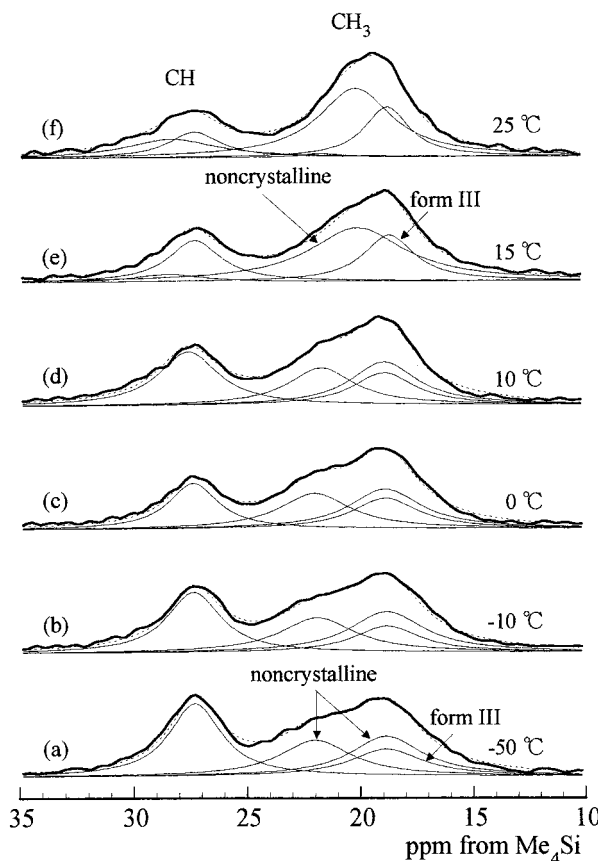


**Figure 5.** Fully relaxed DD/MAS  $^{13}\text{C}$  NMR spectra measured at  $-50$  to  $25$  °C for the form III sample.

readily obtained at different temperatures above 30 °C by the same method as for the case of the form I sample. On the other hand, the line shape analysis for the form III sample below 25 °C is carried out in this paper as shown in Figure 5. Here, the  $\text{CH}_3$  resonance line is found to be composed of the noncrystalline component with the *tt* and *tg* conformations, which respectively corresponds to the  $\text{CH}_3(\text{I})$  and  $\text{CH}_3(\text{II})$  lines, and the form III line with the *tt* conformation. In good accord with the case of the form I sample, the  $\text{CH}_3(\text{I})$  and  $\text{CH}_3(\text{II})$  lines for the noncrystalline component clearly merge into a single line above 15 °C as a result that the *t*–*g* exchange rate attains to about 100 Hz. This analysis also reveals that the degree of crystallinity is 0.31 for the form III sample, and the *trans* fraction of the noncrystalline chains is  $0.76 \pm 0.02$ – $0.78 \pm 0.02$  at  $-50$  to  $25$  °C.

In Figure 6 is plotted the *trans* fraction for the noncrystalline chains obtained for the form I and III samples as described above as a function of temperature. For comparison, the *trans* fraction is also shown for the melt at 170 °C as a square, which is estimated from the chemical shift of the  $\text{CH}_3$  line by using the two-site exchange model as done for the form I and III samples above 15 °C, and for the noncrystalline sample at 0 °C as a triangle just after quenched from the melt as described above. As is typically seen for the form I sample, there are three regions, regions A, B, and C in the order of increasing temperature. In region A, which corresponds to the temperature region below 15 °C, the *trans* fraction is extraordinarily high for the noncrystalline chains in the respective samples as already pointed out. Moreover, such a high *trans* fraction seems to depend on the degree of crystallinity: the noncrystalline

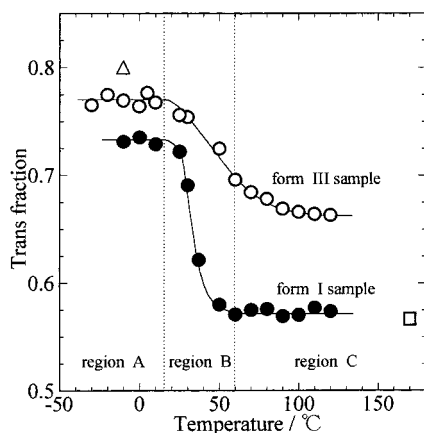


**Figure 6.** Temperature dependence of the *trans* fraction of the noncrystalline component for the form I and II samples, estimated from the  $\text{CH}_3$  resonance line.  $\Delta$  and  $\square$  indicate the *trans* fractions in the noncrystalline state at 0 °C and at the melt at 170 °C, respectively.

sample has the highest value, whereas the form I sample with the highest crystallinity gives the lowest. The existence of crystallites may reduce the probability of the *trans*-rich conformation thermodynamically allowable for the noncrystalline chains in region A probably due to the limited space. The effects of the existence of a solvent on the *trans* fraction for sPP will be also reported elsewhere.<sup>30</sup>

In contrast, the *trans* fraction for the form I sample in region C is of the same level as expected for the melt, suggesting that the noncrystalline chains are fully relaxed above 60 °C and adopt the almost random conformation. As far as in region C, fully relaxed sPP chains can be assumed to behave like conventional vinyl polymers. However, there is still some restriction in the noncrystalline region for the form III sample in region C as is evidently seen from the higher *trans* fraction compared to that for the form I sample or for the melt. Above 60 °C, form I is newly crystallized as a result of partial melting of form III crystallites in the form III sample as previously reported.<sup>20</sup> The restriction produced in the noncrystalline region by the aggregates of the *trans*-rich noncrystalline segments will not be fully relaxed in the successive process of partial melting of form III and the crystallization of form I.

Region B is the transitional region existing between regions A and B, where the *trans* fraction is greatly changed as is typically observed for the form I sample. Such a drastic conformational change may not be interpreted simply in terms of the intramolecular interaction for a single sPP chain, but by considering the intermolecular interaction associated with plural chains that is not yet characterized for sPP chains at present. In this sense, the drastic conformational change in region B will be named as *trans*-rich chain assembly-coiled chains transition. In the *trans*-rich chain assembly each sPP chain may rather weakly aggregate with each other because the respective C–C bonds are subjected to the rapid *t*–*g* exchange, for example, with a frequency of about 100 Hz even at 15 °C as described above.

On the other hand, it has already been reported by the similar analysis of the  $^{13}\text{C}$  chemical shift value for the  $\text{CH}_2$  line that the *trans* fraction of the noncrystalline component is as high as 0.79 even above about 50 °C for sPP with somewhat lower syndiotacticity than ours.<sup>24</sup> Since this fact seems to be in conflict with the

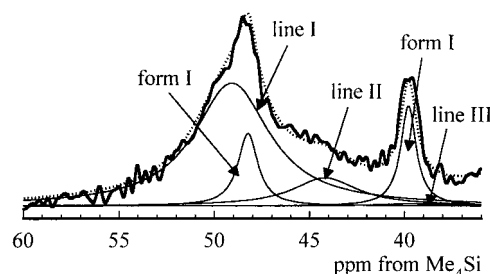


**Figure 7.** Line shape analysis for the  $\text{CH}_2$  resonance line measured at 10 °C by the  $\pi/2$  single pulse sequence with a pulse delay time of 12 s. Here, the noncrystalline contribution composed of lines I, II, and III reflects the equilibrium magnetization because the  $T_{1C}$  value is of the order of 2.2 s.

marked conformational change above about 15 °C shown in Figure 6, we have also determined the *trans* fraction by analyzing the  $^{13}\text{C}$  chemical shift value of the  $\text{CH}_2$  line for the form I sample at each temperature ranging from 10 to 120 °C. As an example, Figure 7 shows the  $\text{CH}_2$  resonance line measured at 10 °C by the  $\pi/2$  single pulse sequence with a pulse delay time of 12 s and constituent lines for the crystalline and noncrystalline components obtained by the least-squares line shape analysis. Here, the noncrystalline contribution reflects the equilibrium magnetization, because its  $T_{1C}$  is found to be 2.2 s at 10 °C. Two resonance lines assignable to the form I crystals appear at about 48 and 40 ppm, in good accord with the previous results.<sup>5,24</sup> It is also confirmed that lines I, II, and III ascribed to the noncrystalline component appear at the same positions as the corresponding lines for the quenched sPP sample shown in Figure 2. Accordingly, the *trans* fraction should be determined to be 0.90 from the integrated fractions of lines I, II, and III, which are estimated to be 0.82, 0.17, and 0.01, respectively. In contrast, these three lines merge into a single line above about 20 °C, like the case of the  $\text{CH}_3$  resonance line shown in Figures 4 and 5, as a result of the rapid *t*–*g* exchange motion. In these cases, therefore, motionally averaged chemical shift values are readily obtained for the noncrystalline component in the spectra measured at different temperatures under the same condition as for the case shown in Figure 7. The *trans* fractions are determined from the chemical shift values thus obtained by using the three-site exchange model under the assumption of the Bernoulli statistics for the *trans* and *gauche* distributions.<sup>24</sup>

In Figure 8, the *trans* fractions thus obtained for the noncrystalline  $\text{CH}_2$  resonance line are plotted against temperature. Interestingly, the *trans* fraction is as high as about 0.9 in this temperature region including the melt indicated by the open square, and there is no significant conformational change unlike the results for the  $\text{CH}_3$  resonance lines shown in Figure 6. These results are in good accord with the previous result<sup>24</sup> that the *trans* fraction stays 0.79 in that sample even above about 50 °C. In Figure 8 the *trans* fraction is also shown for the quenched noncrystalline sample as a triangle, which was obtained by the line shape analysis shown in Figure 2. This value is significantly lower than the value obtained for the noncrystalline component involved in the form I sample. The cause of such a difference in *trans* fraction is not clear at present, although it may be due to the existence of crystallites.

The results independently obtained in Figures 7 and 8 seem to be in conflict with each other from the

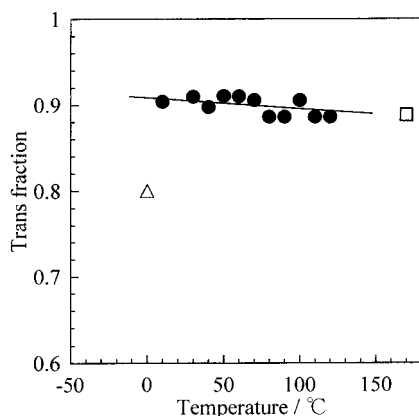


**Figure 8.** Temperature dependence of the *trans* fraction of the noncrystalline component for the form I sample, estimated from the CH<sub>2</sub> resonance line.  $\Delta$  and  $\square$  indicate the *trans* fractions in the noncrystalline state at 0 °C and at the melt at 170 °C, respectively.

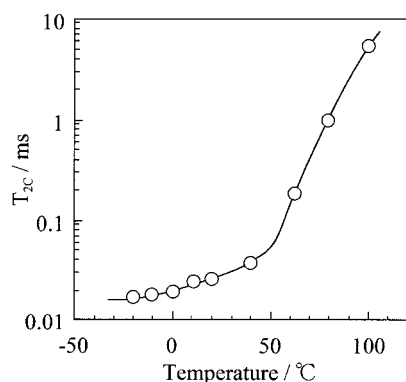


**Figure 9.** Temperature dependence of the <sup>13</sup>C spin–spin relaxation time (*T*<sub>2C</sub>) for the noncrystalline CH line at 27 ppm for the form I sample.

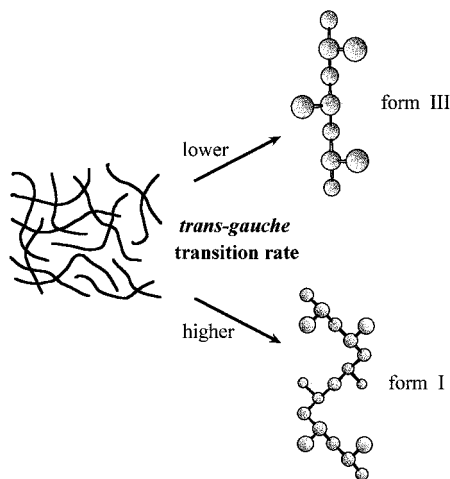
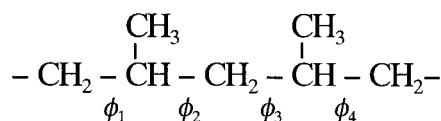


**Figure 10.** Schematic drawing for the crystallization process of form I or form III in region A.

Bernoulli statistics viewpoint. As shown in Table 1, the chemical shift value of the CH<sub>2</sub> carbon is determined by the conformations of bonds 1 and 4, whereas the value of the CH<sub>3</sub> carbon depends on the conformations for bonds 1 and 2 or bonds 3 and 4. On the basis of the results shown in Figures 7 and 8, all possible conformations for four successive sPP bonds and their mole fractions in regions A and C are also shown in Table 1. Here, the latter mole fractions have been calculated from the *tt* and *tg* fractions estimated from the CH<sub>3</sub>

**Table 1.** Possible Conformations for Four Successive Main Chain Bonds of sPP and Their Mole Fractions Estimated from the <sup>13</sup>C Chemical Shift Values of the CH<sub>3</sub> Resonance Lines in Regions A and C



conformation <sup>a</sup>				mole fraction <sup>b</sup>	
$\phi_1$	$\phi_2$	$\phi_3$	$\phi_4$	region A <sup>c</sup>	region C <sup>d</sup>
<i>t</i>	<i>t</i>	<i>t</i>	<i>t</i>	0.36	0.02
<i>t</i>	<i>t</i>	<i>t</i>	<i>g</i>	0.12	0.06
<i>t</i>	<i>t</i>	<i>g</i>	<i>t</i>	0.12	0.06
<i>t</i>	<i>g</i>	<i>t</i>	<i>t</i>	0.12	0.06
<i>t</i>	<i>g</i>	<i>t</i>	<i>g</i>	0.04	0.185
<i>t</i>	<i>g</i>	<i>g</i>	<i>t</i>	0.04	0.185
<i>g</i>	<i>t</i>	<i>t</i>	<i>t</i>	0.12	0.06
<i>g</i>	<i>t</i>	<i>t</i>	<i>g</i>	0.04	0.185
<i>g</i>	<i>t</i>	<i>g</i>	<i>t</i>	0.04	0.185

<sup>a</sup> Determined from the CH<sub>2</sub> and CH<sub>3</sub> resonance lines. <sup>b</sup> Estimated from the integrated fractions of lines I and II for the CH<sub>3</sub> carbons, which are assigned to *tg* and *tt* for  $\phi_1$  and  $\phi_2$  (or  $\phi_3$  and  $\phi_4$ ), respectively. <sup>c</sup> Below about 15 °C as shown in Figure 6. <sup>d</sup> Above about 60 °C as shown in Figure 6.

resonance lines for the noncrystalline sample without crystallites in regions A and C. According to this calculation, the mole fractions of *t@t*, *t@g+g@t*, and *g@g* conformations are 0.64, 0.32, and 0.04 in region A, respectively. These values are significantly deviated from the corresponding values, 0.82, 0.17, and 0.01, experimentally obtained from the CH<sub>2</sub> resonance line shown in Figure 7. Moreover, such differences are enhanced in region C; the former mole fractions expected by the calculation in Table 1 are 0.265, 0.305, and 0.185, while the latter fractions experimentally obtained stay almost constant even in region C. These facts may be mainly due to a much less probability of the *gttg* conformation and inversely due to a much higher probability of the *tggt* conformation compared to the probabilities expected from the simple Bernoulli statistics. Such different distributions of the conformations should stem from the intramolecular steric hindrance between the CH<sub>3</sub> groups including the second and third neighbors in regions A and C as well as probably from some sort of intermolecular interaction to induce molecular assemblies in region A. Since the similar conformational change shown in Figures 7 and 8 was also observed for atactic polypropylene, a molecular dynamics simulation is in progress to reproduce such a conformational change in the simulation and to clarify the intramolecular and intermolecular origins.

To examine the change in molecular mobility for the noncrystalline chains appearing as a result of the *trans-rich chain assembly-coiled chains* transition, <sup>13</sup>C spin–spin relaxation times (*T*<sub>2C</sub>) were measured at different temperatures for the form I sample by the spin-echo pulse sequence modified for solid-state measurements.<sup>29,31,32</sup> The form I sample is more suitable for this experiment compared to the form III sample because there is almost no change in morphological structure at this temperature range, and the transition is more clearly observed. <sup>1</sup>H gated dipolar decoupling was employed only during the period of the FID acquisition. To suppress the contribution from the crystalline component, the noncrystalline CH line at 27 ppm was used, and the pulse delay time for the FID accumulation was set to 2.0 s. An almost single-exponential decay curve

was obtained at each temperature. Figure 7 shows the temperature dependence of  $T_{2C}$  thus obtained for the noncrystalline component in the form I sample. It is found that the  $T_{2C}$  value is more rapidly increased above about 50 °C, whereas the value stays at the level lower than several tens of microseconds. This fact indicates that the molecular mobility of the noncrystalline sPP chains attains to the level for the rubbery component for polyethylene<sup>29,31</sup> at room temperature in region C, whereas the chains are significantly limited in molecular mobility in regions A and B.

**Hypothesis for the Crystallization of Form III and Form I.** When sPP is crystallized from the melt by slowly cooling, it is well-known that form I composed of antichiral helices with the *ttgg* conformation is produced in good accord with the prediction by the theoretical calculation<sup>8</sup> that the most stable crystal structure for sPP is form I. This must be the typical crystallization of sPP in region C where the noncrystalline chains adopt the relatively random conformation. In contrast, form III with the planar zigzag conformation seems to be preferentially crystallized in region A where the *trans* fraction is as high as 0.8–0.9 in the noncrystalline state before the crystallization starts. In fact, form III is found to be exclusively produced at 0 °C after quenched from the melt. Nevertheless, recent FT-IR measurements<sup>3</sup> revealed that form I is allowed to be crystallized above about 5 °C even in region A, and the degree of crystallinity of form I is significantly increased with increasing crystallization temperature. In contrast, form III is greatly reduced in degree of crystallinity with increasing temperature, and the crystallization of this form finally stops above about 16 °C even in region A. This fact indicates that the high *trans* fraction of the noncrystalline sPP chains is not the main factor to determine the crystal form to be produced at a certain temperature in region A.

As is already described, the *t*–*g* exchange rate for the *trans*-rich noncrystalline chains attains to the level of 100 Hz at about 15 °C. This dynamic factor may be additionally important in the crystallization in region A. When the *t*–*g* exchange rate is less than about 100 Hz, sPP chains may be preferable to the crystallization of form III as is schematically shown in Figure 8. The reason will be that the planar zigzag parts in possible *trans*-rich chain assemblies may aggregate with each other at a higher probability to create the nuclei for form III crystallites when the *t*–*g* exchange rate is lower than about 100 Hz. In contrast, when the exchange rate becomes higher than about 100 Hz, local conformations averaged in a given period must be more randomized. Such a situation may be preferable to the nucleation of form I crystallites with the *ttgg* conformation. More detailed characterization of the dynamic factor affecting the crystallization in region A is in progress, including the examination of effects of the tacticity of polypropylene chains.

## Conclusion

Conformational changes for the sPP noncrystalline chains were investigated at different temperatures by high-resolution solid-state <sup>13</sup>C NMR spectroscopy to understand the mechanism of the spontaneous crystallization of the planar zigzag form (form III) around 0 °C, and the following conclusions were obtained:

(1) To suppress the crystallization of form I, the noncrystalline sPP sample which was quenched at 0 °C

from the melt was further cooled to –20 °C, and the fully relaxed DD/MAS <sup>13</sup>C NMR spectrum was obtained by the  $\pi/2$  single pulse sequence. The line shape analysis considering the  $\gamma$ -gauche effect for the CH<sub>2</sub> resonance line revealed that the *trans* fraction is as high as 0.80, in good accord with the previous result obtained by the similar analysis for the CH<sub>3</sub> resonance line. It was also found that the *gg* conformation is allowed for the CH(CH<sub>3</sub>)–CH<sub>2</sub>–CH(CH<sub>3</sub>) sequence as statistically expected although this conformation is completely inhibited for the CH<sub>2</sub>–CH(CH<sub>3</sub>)–CH<sub>2</sub> sequence.

(2) It is very important to determine the *trans* fraction of the noncrystalline sPP chains as a function of temperature to know the cause of the high *trans* fraction at 0 °C in the noncrystalline state. To this end, samples containing form I and III crystallites were crystallized at 100 °C for 24 h and 0 °C for 144 h, respectively. The same line shape analysis previously reported was successfully performed for the CH<sub>3</sub> resonance lines in fully relaxed DD/MAS <sup>13</sup>C NMR spectra obtained for those samples at different temperatures.

(3) The *trans* fraction thus obtained for the noncrystalline component in each sample was plotted as a function of temperature. As a result, it was found there are three regions, regions A, B, and C, where the *trans* fractions are greatly different. In region A, which corresponds to the temperature region below about 15 °C, the *trans* fraction was as high as 0.73–0.80 depending on the degree of crystallinity, whereas this fraction was the ordinary level (~0.57) in region C appearing above 60 °C as observed at the melt. In region B, which is the transitional region between regions A and C, the *trans* fraction should be markedly altered with temperature. Since such a conformational change seemed not to be interpreted only in terms of the intramolecular interaction for a single chain, this transition was named as *trans*-rich chain assembly–coiled chains transition.

(4) In contrast, no significant conformational change was observed for the results obtained by the similar analysis for the CH<sub>2</sub> noncrystalline resonance line for the form I sample, although the *trans* fraction was also as high as about 0.9 at temperatures ranging from 10 to 170 °C. This fact suggests that the simple Bernoulli statistics is not fulfilled for the distributions of the *trans* and *gauche* conformations in the noncrystalline region for sPP, and the *tggt* conformation may be preferably produced for the CH<sub>2</sub>–CH(CH<sub>3</sub>)–CH<sub>2</sub>–CH(CH<sub>3</sub>)–CH<sub>2</sub> bonds under the suppression of the *gttg* conformation mainly as a result of the steric hindrance between the CH<sub>3</sub> groups including the second and third neighbors.

(5)  $T_{2C}$  values were measured for the noncrystalline component in the form I sample at different temperatures by the spin-echo pulse sequence modified for solid-state measurements. As a result, it was found that the molecular motion is highly restricted in regions A and B, while the noncrystalline component in region C undergoes much enhanced motion as observed for the rubbery component in polyethylene samples.

(6) In region A, form III with the planar zigzag conformation is spontaneously crystallized, and the maximum degree of crystallinity is obtained at about 0 °C. The most stable form (form I), which is composed of antichiral helices with the *ttgg* conformation, is also crystallized above about 5 °C in region A, although this form is preferentially produced in regions B and C. Therefore, the high *trans* fraction is not a single essential factor affecting the crystallization of form I in

region A. Since the  $t$ - $g$  exchange rate of the noncrystalline chains was found to attain to about 100 Hz at about 15 °C, such a dynamic factor should be considered as an additional factor determining the crystal form produced in region A.

**Acknowledgment.** We are grateful to Drs. Hitoshi Miura and Hiroaki Katayama of Sumitomo Chemical Co. Ltd. for kindly providing the highly syndiotactic polypropylene sample.

## References and Notes

- (1) Nakaoki, T.; Ohira, Y.; Hayashi, H.; Horii, F. *Macromolecules* **1998**, *31*, 2705.
- (2) Ohira, Y.; Horii, F.; Nakaoki, T. *Macromolecules* **2000**, *33*, 1801.
- (3) Nakaoki, T.; Yamanaka, T.; Ohira, Y.; Horii, F. *Macromolecules* **2000**, *33*, 2718.
- (4) Tadokoro, H.; Kobayashi, M.; Kobayashi, S.; Yasufuku, K.; Mori, K. *Rep. Prog. Polym. Phys. Jpn.* **1966**, *9*, 181.
- (5) Sozzani, P.; Simonutti, R.; Comotti, A. *Magn. Reson. Chem.* **1994**, *32*, s45.
- (6) Asakura, T.; Aoki, A.; Date, T.; Demura, M.; Asanuma, T. *Polym. J.* **1996**, *28*, 24.
- (7) De Rosa, C.; Auriemma, F.; Vinti, V. *Macromolecules* **1998**, *31*, 7430.
- (8) Natta, G.; Corradini, P.; Ganis, P. *Makromol. Chem.* **1960**, *39*, 238.
- (9) Natta, G.; Peraldo, M.; Allegra, G. *Makromol. Chem.* **1964**, *75*, 215.
- (10) Chatani, Y.; Maruyama, H.; Noguchi, K.; Asanuma, T.; Shiomura, T. *J. Polym. Sci., Polym. Phys. Lett.* **1990**, *28*, 393.
- (11) Sozzani, P.; Galimberti, M.; Balbontin, G. *Makromol. Chem. Rapid Commun.* **1992**, *13*, 305.
- (12) Corradini, P.; Natta, G.; Ganis, P.; Temussi, P. A. *J. Polym. Sci., Part C* **1967**, *16*, 2477.
- (13) Lovinger, A. J.; Davis, D. D.; Lotz, B. *Macromolecules* **1991**, *24*, 552.
- (14) Lovinger, A. J.; Lotz, B.; Padden, F. J. *Macromolecules* **1993**, *26*, 3494.
- (15) De Rosa, C.; Corradini, P. *Macromolecules* **1993**, *26*, 5711.
- (16) De Rosa, C.; Auriemma, F.; Corradini, P. *Macromolecules* **1996**, *29*, 7452.
- (17) Auriemma, F.; Lewis, R. H.; Spiess, H. W.; De Rosa, C. *Macromol. Chem. Phys.* **1995**, *196*, 4011.
- (18) De Rosa, C.; Auriemma, F.; Vinti, V. *Macromolecules* **1997**, *30*, 4137.
- (19) Auriemma, F.; De Rosa, C.; Ruiz de Ballesteros, O.; Corradini, P. *Macromolecules* **1997**, *30*, 6586.
- (20) Ohira, Y.; Horii, F.; Nakaoki, T. *Macromolecules* **2000**, *33*, 5566.
- (21) Kaplan, M. L.; Bovey, F. A.; Chang, H. V. *Anal. Chem.* **1975**, *47*, 1703.
- (22) English, A. D. *J. Magn. Reson.* **1984**, *57*, 491.
- (23) Murata, T.; Horii, F.; Fujito, T. *Proc. Soc. Solid-State NMR Polym.* **1990**, No. 7, 29.
- (24) Sozzani, P.; Simonutti, R.; Galimberti, M. *Macromolecules* **1993**, *26*, 5782.
- (25) Abragam, A. *The Principles of Nuclear Magnetism*; Clarendon Press: Oxford, 1989; p 450.
- (26) Suwelack, D.; Rothwell, W. P.; Waugh, J. S. *J. Chem. Phys.* **1980**, *73*, 2559.
- (27) Rothwell, W. P.; Waugh, J. S. *J. Chem. Phys.* **1981**, *74*, 2721.
- (28) Takegoshi, K.; Hikichi, K. *J. Chem. Phys.* **1991**, *94*, 3200.
- (29) Kuwabara, K.; Kaji, H.; Horii, F. *Macromolecules* **2000**, *33*, 4453.
- (30) Nakaoki, T.; Ohira, Y.; Horii, F. *Polymer*, in press.
- (31) Kitamaru, R.; Horii, F.; Murayama, K. *Macromolecules* **1986**, *19*, 636.
- (32) Hirai, A.; Horii, F.; Kitamaru, R.; Fatou, J. G.; Bello, A. *Macromolecules* **1990**, *23*, 2913.

MA0014564